Journal of Physics: Conference Series **572** (2014) 012057 doi:10.1088/1742-6596/572/1/012057

Computation of wall bounded flows with heat transfer in the framework of SRS approaches

M S Gritskevich[1], A V Garbaruk[1], F R Menter[2]

[1]St. Petersburg State Polytechnical University, 195251, St. Petersburg, Russia
[2]Software Development Department, ANSYS, 83714, Otterfing, Germany

E-mail: gritckevich@gmail.com

Abstract. A detailed assessment of Scale Adaptive Simulation (SAS) and Improved Delayed Detached Eddy Simulation (IDDES) is performed for prediction of heat transfer for several wall bounded flow. For that purpose a zero pressure gradient boundary layer, a backward facing step, and a thermal mixing in a T-Junction test cases are considered. The results, obtained with the use of ANSYS-FLUENT, show that both approaches are capable to predict both mean and RMS velocity and temperature with sufficient accuracy.

1. Introduction

A prediction of heat transfer for unsteady wall bounded flows is a challenging task for Computational Fluid Dynamics (CFD). CFD methods based on Unsteady Reynolds Averaged Navier-Stokes (URANS) equations, which are typically used in industrial applications, have difficulties in providing accurate mean solution and are almost incapable to predict RMS velocity and temperature. Thus, in many cases, high turbulent viscosity, predicted by URANS models, suppresses development of any transient flow and a steady-state solution is obtained. From the other point, Scale Resolving Simulations (SRS) are able to provide such information with sufficient accuracy but requires large computational resources, which are beyond the capabilities of modern computers. Nevertheless, recent studies (e.g. [1]) have shown promising results for such flows with the use of some advanced SRS approaches. However, a detailed validation of these methods is still required in order to determine their accuracy and range of validity. For that purpose, two modern SRS approaches are considered, namely Scale Adaptive Simulation (SAS) [2] and Improved Delayed Detached Eddy Simulation (IDDES) [3], which are used in conjunction with inflow turbulent content generated with either Vortex Method (VM) [4] or Generator of Synthetic Turbulence (GST) [5,6].

2. Results and Discussions

Three test cases are considered within the paper. A zero pressure gradient boundary layer is a benchmark test case, for which a number of correlations for both velocity and temperature are available for different Reynolds and Prandtl numbers (e.g. [7]). A backward facing step flow [8] includes both separation and reattachment and is often used as a stress test for SRS approaches. Characteristic feature of a thermal mixing in a T-Junction flow [9] is a so-called “thermal striping” effect, which arise due to temperature fluctuation and, therefore, cannot be handled by conventional URANS approaches [1].

All the simulations within the paper have been carried out with the use of ANSYS-FLUENT [10]. Within this code a finite volume method on unstructured grids with a cell-centered data arrangement is applied to governing transient equations. Inviscid fluxes are approximated with the use of second order centered scheme for momentum equations and with the use of second order upwind scheme for temperature and turbulence equations. Time derivatives are discretized with the use of three-level second order backward scheme.

2.1. Zero Pressure Gradient Boundary Layer

Simulations of this flow are carried out at two Reynolds numbers $Re_\delta=\rho\cdot U_0\cdot\delta_0/\mu=130$ and $Re_\delta=1300$ (U_0 is a free stream velocity, δ_0 is a boundary layer thickness at the inlet section, ρ is a constant density, and μ is a constant dynamic viscosity). For each Reynolds number two Prandtl numbers $\mathrm{Pr}=\mu\cdot C_p/\lambda=0.64$ and $\mathrm{Pr}=6.4$ are considered (C_p is a constant specific heat capacity and λ is a constant thermal conductivity). The free-stream flow and the wall are maintained at constant temperature of $T_0=300$ K and $T_0+\Delta T$ ($\Delta T=10$ K) respectively.

A computational domain (Figure 1) is a box with dimensions of $31.25\delta_0\times12.5\delta_0\times3.875\delta_0$ in streamwise, wall-normal and spanwise directions respectively. A computational grid (Figure 1) has $1.1\cdot10^6$ cells for $Re_\delta=130$ and $1.3\cdot10^6$ cells for $Re_\delta=1300$. The grid steps are equal to $\Delta x=0.125\cdot\delta_0$ and $\Delta z=0.0625\cdot\delta_0$ in streamwise and spanwise directions respectively. In wall units this corresponds to $\Delta x^+=60$ and $\Delta z^+=30$ for $Re_\delta=130$ and to $\Delta x^+=450$ and $\Delta z^+=225$ for $Re_\delta=1300$. The grid has a dense clustering towards the wall to satisfy $\Delta y^+<1$ for both Reynolds numbers. A non-dimensional time step of $\Delta t=0.03\cdot\delta_0/U_0$ is applied, which ensures the CFL number to be less than one in the entire domain. Unsteady statistics is obtained by averaging of instantaneous flow fields over 5000 time steps.

Boundary conditions are shown in Figure 1. Inlet profiles are obtained from a precursor SST-RANS simulation of a boundary layer flow up to specified δ_0 and are then used for generation of inflow turbulent content with the use of GST [5,6]. A symmetry condition is specified on the upper boundary. No-slip condition with a constant temperature of $T_0+\Delta T$ is specified on the wall. Periodic condition is applied in spanwise direction. On the outlet boundary a constant pressure is specified, while the rest quantities are extrapolated from the adjacent cells.

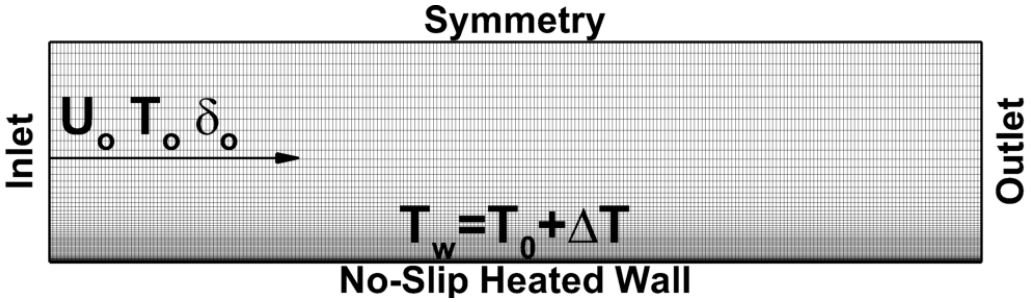

Figure 1. Computational domain and grid for the boundary layer flow

The results of the simulations are shown in Figure 2 and in Figure 3. As seen both IDDES and SAS are in a good agreement with the correlation [7] for both Reynolds numbers and for both Prandtl numbers. Therefore, both approaches are capable to predict this flow with sufficient accuracy.

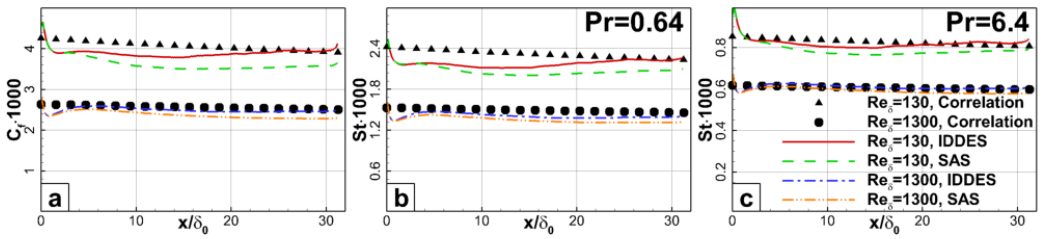

Figure 2. Skin friction coefficient (a) and Stanton number (b, c) distributions at different Reynolds and Prandtl numbers for the boundary layer flow

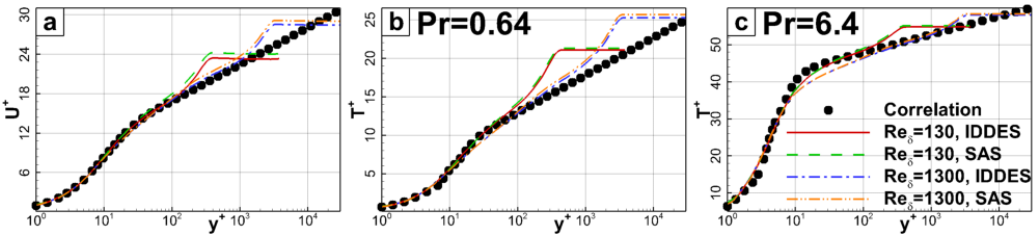

Figure 3. Velocity (a) and temperature (b, c) profiles at different Reynolds and Prandtl numbers for the boundary layer flow

2.2. Backward Facing Step

This flow has been experimentally studied by Vogel and Eaton [8] for $Re=\rho \cdot U_0 \cdot H/\mu=28000$ (U_0 is a bulk velocity at the inlet section, H is a step height, ρ is a constant density, and μ is a constant dynamic viscosity) and for $Pr=\mu \cdot C_p/\lambda=0.7$ (C_p is a constant specific heat capacity and λ is a constant thermal conductivity). An expansion ratio of the upstream plane channel is 1.25, in which a flow is held at constant temperature of T_0=300 K. The lower wall is heated with a constant flux of $Q_w=1.44 \cdot \lambda \cdot T_0/H$, while on the rest walls adiabatic condition are maintained.

A computational domain (Figure 4) for this test case is similar to those used in [3]. In streamwise direction is extends from $-3.8 \cdot H$ to $20 \cdot H$ ($x/H=0$ corresponds to the step location), while in spanwise direction it has a size of $4 \cdot H$. A computational grid (Figure 4) consists from $2.8 \cdot 10^6$ hexahedral cells. The maximum grid steps in streamwise and spanwise directions are equal to $0.1 \cdot H$ and to $0.05 \cdot H$ respectively, which corresponds to $\Delta x^+=200$ and to $\Delta z^+=100$ in wall units. The gird steps in wall normal direction correspond to $\Delta y^+<1$ in the entire domain. A non-dimensional time step of $\Delta t=0.02 \cdot H/U_0$ ensures the CFL number of less than one. Instantaneous flow fields are averaged over 5000 time steps and a sufficient time sample for unsteady statistics is achieved.

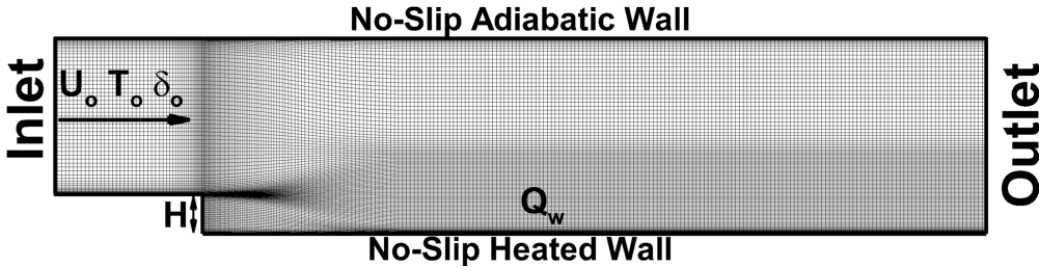

Figure 4. Computational domain and grid for the backward-facing step flow

Boundary conditions are specified as follows (Figure 4). The inflow profiles are obtained from a precursor SST-RANS simulation of a developing plane channel flow up to experimental boundary layer thickness of $\delta_0=H$ and are then used for the GST generator [5,6]. Periodic condition is specified in spanwise direction. No-slip condition is specified on solid walls. On the lower wall a constant heat flux of Q_w is specified, while on the rest walls adiabatic condition is applied. On the outlet boundary a constant pressure is specified, while the rest quantities are extrapolated from the domain.

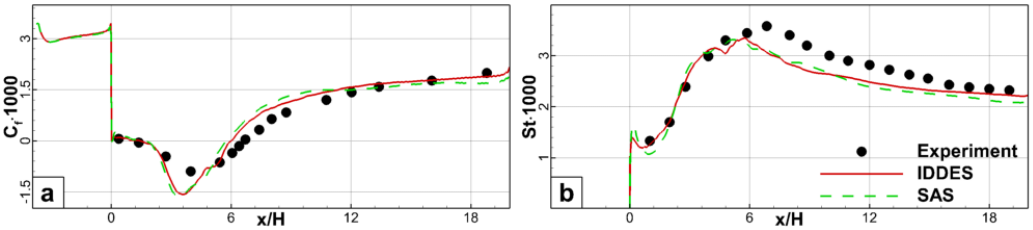

Figure 5. Skin friction coefficient (a) and Stanton number (b) distributions for the backward facing step flow

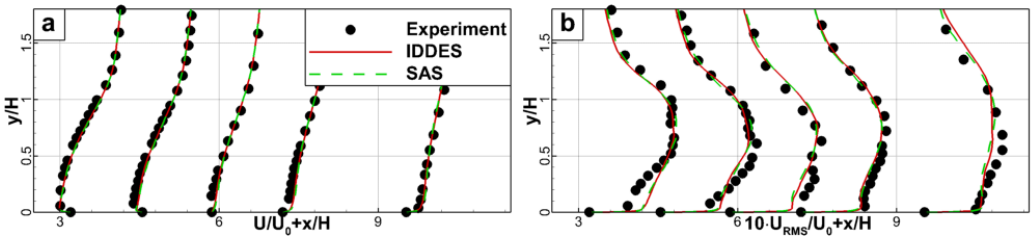

Figure 6. Mean (a) and RMS (b) velocity profiles for the backward facing step flow. The profiles are plotted at x/H=3.2, 4.55, 5.86, 7.2, and 9.53

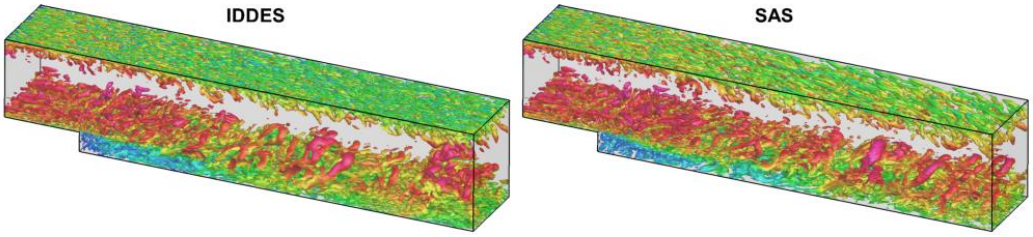

Figure 7. Instantaneous isosurfaces of Q-criterion coloured with contours of velocity magnitude for the backward facing step flow

As seen from distributions of skin friction coefficient and Stanton number (Figure 5) both considered models yield virtually identical results and agree fairly well with the experimental data [8]. Similar trend is also observed for mean and RMS velocity profiles (Figure 6) and for instantaneous isosurfaces of Q-criterion (Figure 7). Thus, both approaches are capable to predict both flow and heat transfer with sufficient accuracy.

2.3. Thermal mixing in T-Junction

A thermal mixing of water in a T-Junction has been experimentally studied in [9]. The setup (Figure 8) consists of vertical and horizontal pipes with an inner diameter of D_0 and $1.4 \cdot D_0$ respectively. The length of the straight pipes upstream of the T-Junction is more than $110 \cdot D_0$ for the horizontal pipe and about $20 \cdot D_0$ for the vertical pipe. A constant mass flow and temperature is kept throughout the experiment in both pipes with velocity and temperature equal to U_0 and T_0=309 K in the vertical pipe and to $0.76 \cdot U_0$ and T_0-ΔT (ΔT=17 K) in the horizontal pipe. These parameters correspond to $Re=\rho \cdot U_0 \cdot D_0/\mu=8 \cdot 10^4$ (ρ is a constant density and μ is a dynamic viscosity, calculated based on a temperature field according to [9]) and to $Pr=\mu \cdot C_p/\lambda=5$ (C_p is a constant specific heat capacity and λ is a constant thermal conductivity).

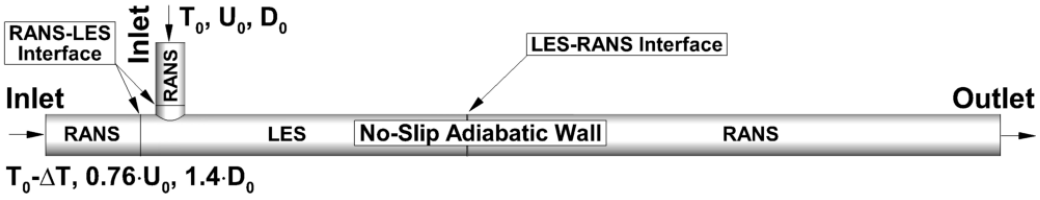

Figure 8. Computational domain for the T-Junction flow

Parameters of computational domain and grid are similar to those used in [1]. The computational domain is shown in Figure 8. The inlet sections are located at z/D_0=3.1 in the vertical pipe and at x/D_0=-4.2 and the horizontal pipe. The outlet section is located at x/D_0=28.0. The computational grid consists of about $4.9 \cdot 10^6$ hexahedral cells. The maximum grid steps in axial (Δ_a) and circumferential (Δ_c) directions are Δ_a/D_0=0.036 and Δ_c/D_0=0.018 respectively, which corresponds to Δ_a^+=7500 and Δ_c^+=4500 in wall units. The size of adjacent to the wall cells corresponds to Δy^+<1 in most of the domain. The used time step is equal to $\Delta t=0.016 \cdot D_0/U_0$ and corresponds to maximum CFL number of

around 4 near the junction. Unsteady statistics is obtained by averaging of instantaneous flow fields over 40000 time steps.

Boundary conditions are shown in Figure 8. The inflow profiles are obtained from a precursor SST-RANS simulation of a pipe flow. For the horizontal pipe a periodic pipe flow is calculated, while for the vertical pipe a calculation of a developing pipe flow up to the experimental value of boundary layer thickness equal to δ_0=0.22·D_0 is performed. No-slip adiabatic condition is applied on pipe walls. A constant pressure is specified on the outlet boundary and the rest quantities are extrapolated from the domain.

For this flow SAS and IDDES are used within an Embedded LES (ELES) approach, according to which the computational domain is decomposed to RANS and LES subdomains as shown in Figure 8. As seen two RANS-LES interfaces at z/D_0=-0.7 and at x/D_0=-1.4 in the vertical and horizontal pipes respectively and one LES-RANS interface at x/D_0=9.8 emerge due to such decomposition. On the RANS-LES interfaces either VM [4] or GST [5,6] are used for generation of turbulent content, while no additional treatment is employed on the LES-RANS interface.

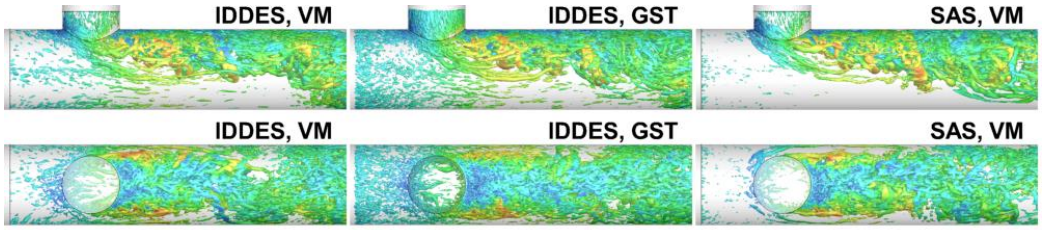

Figure 9. Instantaneous isosurfaces of Q-criterion coloured with contours of velocity magnitude for the T-Junction flow

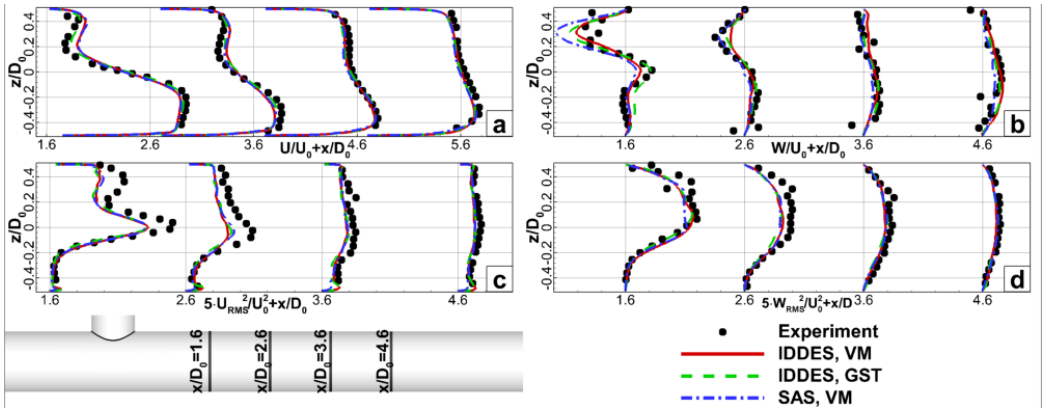

Figure 10. Profiles of mean (a, b) and RMS (c, d) values of velocity for the T-Junction flow. The profiles are show at x/D_0=1.6, 2.6, 3.6, 4.6

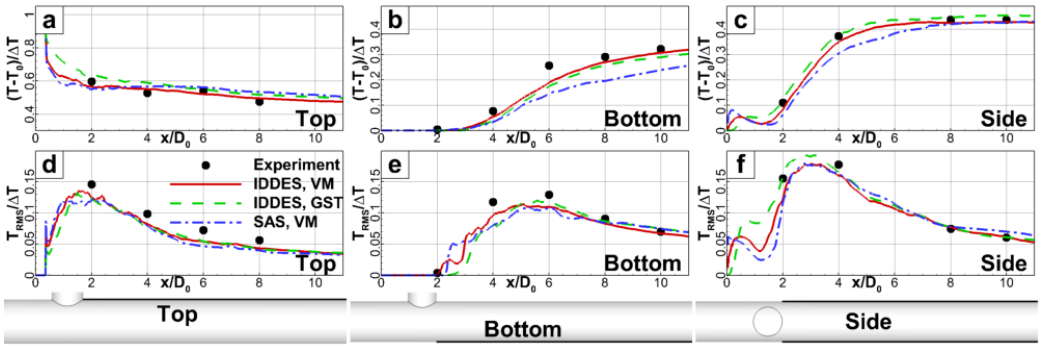

Figure 11. Distributions of mean (a-c) and RMS (d-f) temperature at top, bottom and side sections for the T-Junction flow

As seen from the calculations by SAS and IDDES approaches, instantaneous turbulent structures (Figure 9) are created on the RANS-LES interfaces and are developing downstream. Herewith, the structures obtained with SAS are relatively larger, that those of IDDES. Nevertheless, the presented profiles of mean and RMS velocity (Figure 10) show that both approaches yield virtually identical results that agree fairly well with the experimental data [9]. As regards the distributions of mean and RMS temperature on pipe walls (Figure 11) again good agreement with the experimental data is achieved for all the considered approaches, however, a distribution of mean temperature at bottom section is slightly underestimated for SAS with VM. Nevertheless, all the considered approaches are capable to predict this flow with sufficient accuracy.

3. Summary

A comparative assessment of two modern SRS approaches has been performed. It has been shown, that both approaches are able to predict both mean and RMS values of temperature and velocity when are used in conjunction with inflow turbulent content generators. Among the considered synthetic turbulence generators no advantage has been observed and both VM and GST are able to provide appropriate inflow turbulent content for all the considered flows.

Acknowledgement

The authors from St. Petersburg are partially supported by the Russian Foundation for Basic Research (grants No. 12-08-00256 and No. 14-08-31121)

References

[1] Gritskevich M, Garbaruk A V., Frank T and Menter F R 2012 Investigation of the Thermal Mixing in a T-Junction Flow with Different SRS Approaches *Proceedings of CFD4NRS-4 The Experimental Validation and Application of CFD and CMFD Codes in Nuclear Reactor Technology* pp 1–11

[2] Menter F R and Egorov Y 2010 The Scale-Adaptive Simulation Method for Unsteady Turbulent Flow Predictions. Part 1: Theory and Model Description *Flow Turbulence and Combustion* **85** 113–38

[3] Gritskevich M S, Garbaruk A V., Schütze J and Menter F R 2012 Development of DDES and IDDES Formulations for the k-ω Shear Stress Transport Model *Flow Turbulence and Combustion* **88** 431–49

[4] Mathey F 2008 Aerodynamic noise simulation of the flow past an airfoil trailing-edge using a hybrid zonal RANS-LES *Computers & Fluids* **37** 836–43

[5] Adamian D Y and Travin A K 2011 Improved version of the synthetic eddy method for setting nonstationary inflow boundary conditions in calculating turbulent flows *High Temperature* **49** 704–11

[6] Gritskevich M S and Garbaruk A V 2012 Embedded large eddy simulation with the use of a volume source of turbulent fluctuations *St. Petersburg State Polytechnical University Journal. Physics and Mathematics* **1(141)** 27–36

[7] Kader B A and Yaglom A M 1972 Heat and Mass Transfer Laws for Fully Turbulent Wall Flows *International Journal of Heat and Mass Transfer* **15** 2329–51

[8] Vogel J C and Eaton J K 1985 Combined heat transfer and fluid dynamic measurements downstream of a backward-facing step *ASME Journal of Heat Transfer* **107** 922–9

[9] OECD/NEA 2009 *OECD/NEA: T-Junction Benchmark Specifications, OECD/NEA & Vattenfall*

[10] Mathur S R and Murthy J Y 1997 A pressure-based method for unstructured meshes *Numerical Heat Transfer* **32** 195–215